Indian Journal of Geo Marine Sciences
Vol. 49 (02), February 2020, pp. 192-200

Robust Conditional Probability Constraint Matched Field Processing

Guolei Zhu, Yingmin Wang and Qi Wang*
School of Marine Science and Technology, Northwestern Polytechnical University, Xi'an 710 072, China

[E-mail: flyingscott@nwpu.edu.cn; ywang@nwpu.edu.cn]

Received 07 August 2018; revised 05 October 2018

In order to improve the robustness of Adaptive Matched Field Processing (AMFP), a Conditional Probability Constraint Matched Field Processing (MFP-CPC) is proposed. The algorithm derives the posterior probability density of the source locations from Bayesian Criterion, then the main lobe of AMFP is protected and the side lobe is restricted by the posterior probability density, so MFP-CPC not only has the merit of high resolution as AMFP, but also improves the robustness. To evaluate the algorithm, the simulated and experimental data in an uncertain shallow ocean environment is used. The results show that in the uncertain ocean environment MFP-CPC is robust not only to the moored source, but also to the moving source. Meanwhile, the localization and tracking is consistent with the trajectory of the moving source.

[Keywords: Adaptive Matched Field Processing (AMFP); Posterior probability density; Robustness; Underwater signal processing]

Introduction

Matched field processing (MFP) technology can combine the physical characteristics of underwater acoustic channel and the traditional signal processing algorithm successfully, thus it is widely used in the underwater target passive location and also used in the underwater acoustic parameters inversion, etc. The main method is to use sound propagation model[1] (such as the normal mode model, the parabolic equation, and the ray, etc.) to build a replica vector of the field in the observation sea area, and then match the measured field with the replica to estimate the location of the source or the channel information[2,3]. MFP is mainly divided into two categories: one is the conventional matching field processor (Conventional MFP, CMFP[4]), also known as the Bartlett processor; another is adaptive matched field processor (Adaptive MFP, AMFP), the representative is the minimum variance distortionless response (MVDR) processor[5,6]. Bartlett is robust but with higher sidelobe and it is difficult to separate from mainlobe and sidelobe. MVDR provides maximum array gain in theory, and excellent sidelobe suppression characteristics, but it's performance drop sharply when the underwater acoustic channel model is different with the actual conditions.

In order to get the maximum array gain and improve the robustness of the algorithm at the same time, the domestic and foreign scholars have proposed many tolerance AMFP method based on the MVDR[7-10], such as: the Minimum Variance-Neighborhood Location Constraints (MV-NLC), the Minimum Variance-Environmental Perturbation Constraints (MV-EPC) and the Sector Focusing (SF), etc.

MV-NLC protects the main lobe and overcome the environment mismatch with small-scale position constraints, but the effectiveness of the algorithm relies on the similar degree of the environment mismatch and the position change of the sound source. In waveguide with same sound velocity, the deep sea error often corresponds to the sound source location changes. But other types of environmental mismatch such as sound velocity profile and geoacoustic parameters mismatch is not similar, in this case, the MV-NLC will fail; MV-EPC protect the main lobe by using the first and second order statistical properties of the replica of signal correlation matrix within the scope of environmental parameter perturbation, with heavy computation. SF constructed a projection matrix by multiple replicas in some area, using the projection matrix to eliminate the influence to the MFP made by noise and environment mismatch, but it's difficult to choose the sector size. In addition there are some other robust AMFP algorithms, such as reduced-order MV-EPC, environment perturbation constraints SF, etc.

In order to improve the robustness of the AMFP algorithm, we use Bayesian criterion to deduce posterior probability estimates of location parameters,

then use the posterior probability density to constrain the AMFP, so we can provide a certain degree of main lobe protection and sidelobe suppression to the AMFP, and obtained good tolerance in mismatch environment. We verify the performance of our algorithm by the simulation data of typical mismatch environment "genlmis", which is published in the Naval Research Laboratory seminar in 1993[11]. Finally, through the processing and analysis with the ocean experimental data from SACLANT Research Center in 1993, making comparison of the Bartlett, MVDR and MFP-CPC location capability, verifying the validity and robustness of the MFP-CPC algorithm in the uncertain environment.

Robust MFP in the uncertain environment

Data Model

Assume ω is the frequency of sound source, m is the position parameter(including distance r and depth z), and the sound propagation channel parameter set is ψ, then the sound pressure vector which is received by vertical linear array of N sensors in the frequency domain can be expressed as:

$$\boldsymbol{x}(\omega) = a(\omega)\boldsymbol{s}(\omega, m, \psi) + \boldsymbol{n}(\omega) \quad ...(1)$$

Where, $\boldsymbol{n}(\omega)$ is the noise vector, assumes it's zero mean additive white gaussian noise, $a(\omega)$ is the amplitude of the complex signal, $\boldsymbol{s}(\omega, m, \psi)$ is the channel transmission function. From the Normal mode theory[12-13] can get the function as below:

$$\boldsymbol{s}(\omega, m, \psi) = -\frac{i}{\rho(z_s)\sqrt{8\pi r}} e^{-i\pi/4} \sum_{l=1}^{L} u_l(z_s) u_l(z) \frac{e^{ik_{rl}r}}{\sqrt{k_{rl}}} \quad ...(2)$$

2.2 MVDR

Generally, the output of the MFP $B(m)$ is composed of sampling covariance matrix $\boldsymbol{R}$ and weight vector $\boldsymbol{w}$.

$$B(m) = \boldsymbol{w}(m)^{\mathrm{H}} \boldsymbol{R} \boldsymbol{w}(m) \quad ...(3)$$

Where the sampling covariance matrix $\boldsymbol{R}$ can be expressed by maximum likelihood estimation of K frequency snapshots like data model of Eq.(1)

$$\boldsymbol{R} = \frac{1}{K} \sum_{k=1}^{K} \boldsymbol{x}_k \boldsymbol{x}_k^{\mathrm{H}} \quad ...(4)$$

In order to suppress sidelobe and improve the resolution, an AMFP method is introduced in the paper[5,14,15], known as the minimum variance distortionless response (MVDR) processor. Its mathematical expression is:

$$\min_{\boldsymbol{w}} \boldsymbol{w}^{\mathrm{H}} \boldsymbol{R} \boldsymbol{w}, \text{ s.t. } \boldsymbol{w}^{\mathrm{H}} \boldsymbol{w}_{\mathrm{c}} = 1 \quad ...(5)$$

Here, the $\boldsymbol{w}_{\mathrm{c}} = \boldsymbol{s}(\omega, m, \psi)$ is $N \times 1$ dimension replica vector of the observation direction. As can be seen from mathematical expression of the algorithm, it's structure, a unity gain weight vector of the observation direction to minimize the weighted array output in the other direction, so as to inhibit sidelobe and improve the resolution.

Using Lagrange multiplier method to solve this optimization problem, get the weight vector and the power output of the MVDR are show as below:

$$\boldsymbol{w}_{\mathrm{MVDR}} = \frac{\boldsymbol{R}^{-1}\boldsymbol{w}_{\mathrm{c}}}{\boldsymbol{w}_{\mathrm{c}}^{\mathrm{H}} \boldsymbol{R}^{-1} \boldsymbol{w}_{\mathrm{c}}} \quad ...(6)$$

$$B_{\mathrm{MVDR}} = \frac{1}{\boldsymbol{w}_{\mathrm{c}}^{\mathrm{H}} \boldsymbol{R}^{-1} \boldsymbol{w}_{\mathrm{c}}} \quad ...(7)$$

The MVDR not only has better array gain but also has better mainlobe and sidelobe than the Bartlett, but during underwater acoustic environment perturbation, especially under the condition of high SNR, the AMFP is easy to have a serious "target suppression" phenomenon, so it's much less robustness than the Bartlett.

MFP-CPC

According to the Bayesian criterion, the posterior PDF of the sound source location parameters can be expressed as[16]:

$$p(m \mid \boldsymbol{x}) = \frac{p(\boldsymbol{x} \mid m) p(m)}{p(\boldsymbol{x})} \quad ...(8)$$

Where, $p(m)$ and $p(\boldsymbol{x})$ are respectively, the PDF of the sound source location m and the PDF of the measurement field $\boldsymbol{x}$. When the measurement field $\boldsymbol{x}$ is known, conditional probability density $p(\boldsymbol{x} \mid m)$ is the function of the location parameter m.

For the data model shown in Eq. (1), since the noise of every element of the vertical linear array of N sensors is an independent identically distributed additive white gaussian noise, so we can get the conditional probability density $p(\boldsymbol{x} \mid m)$, that is the likelihood function as expressed below:

$$p(\boldsymbol{x} \mid m) = \frac{1}{(\sqrt{2\pi}\sigma_{\mathrm{n}})^N} \exp\left[-\frac{\left| \boldsymbol{x} - a\boldsymbol{s}(\omega, m, \psi) \right|^2}{2\sigma_{\mathrm{n}}^2} \right] \quad ...(9)$$

Where σ_n^2 is the power of noise.

Let $\partial p(\boldsymbol{x} \mid m) / \partial a = 0$ got the maximum likelihood estimation of a shown as below:

$$\hat{a} = \frac{\boldsymbol{x}^H \boldsymbol{s}(\omega, m, \psi)}{\left|\boldsymbol{s}(\omega, m, \psi)\right|^2} \quad ...(10)$$

Substituting Eq.(10) into Eq.(9) and put $\boldsymbol{s}(\omega, m, \psi)$ shorthand for $\boldsymbol{s}$, yields the likelihood function:

$$p(\boldsymbol{x} \mid m) = \frac{1}{(\sqrt{2\pi}\sigma_n)^N} \exp\left[\frac{\boldsymbol{s}^H \boldsymbol{R}\boldsymbol{s} - |\boldsymbol{x}|^2 \cdot |\boldsymbol{s}|^2}{2\sigma_n^2 \cdot |\boldsymbol{s}|^2}\right] \quad ...(11)$$

Now, get the posterior probability density function(PDF) by Bayesian criterion:

$$p(m \mid \boldsymbol{x}) = \frac{1}{(\sqrt{2\pi}\sigma_n)^N} \exp\left[\frac{\boldsymbol{s}^H \boldsymbol{R}\boldsymbol{s} - |\boldsymbol{x}|^2 \cdot |\boldsymbol{s}|^2}{2\sigma_n^2 \cdot |\boldsymbol{s}|^2}\right] \cdot \frac{p(m)}{p(\boldsymbol{x})} \quad ...(12)$$

Assume that in the observation sea area, the appearance probability of the target is equal, that is $p(m)$ is constant. When the prior PDF $p(\boldsymbol{x})$ is unknown, in order to ensure the integral of the posterior PDF equal to 1, that is:

$$\sum_m p\left(m \mid x\right) = 1 \quad ...(13)$$

We defined a normalization constant C_x, then get the constant C_x as below:

$$C_x = \frac{1}{\sum_m \exp\left[\frac{\boldsymbol{s}^H \boldsymbol{R}\boldsymbol{s} - |\boldsymbol{x}|^2 \cdot |\boldsymbol{s}|^2}{2\sigma_n^2 \cdot |\boldsymbol{s}|^2}\right]} \quad ...(14)$$

So after we got the posterior PDF of the location parameters, we can construct the MFP as Eq.(15), named as MFP with Conditional Probability Constraint(MFP-CPC):

$$B_{CPC} = p(m \mid \boldsymbol{x}) \cdot B_A = C_x \exp\left[\frac{\boldsymbol{s}^H \boldsymbol{R}\boldsymbol{s} - |\boldsymbol{x}|^2 \cdot |\boldsymbol{s}|^2}{2\sigma_n^2 \cdot |\boldsymbol{s}|^2}\right] \cdot B_A \quad ...(15)$$

Where, B_A is the power output of AMFP. From the output expression of MFP-CPC, it's clear that the MFP-CPC uses prior knowledge about the environment and introduce the Bayesian criteria to the algorithm, is a kind of combining method by data driven and the base model; Take the AMFP as the basic unit, the algorithm has general expression. In this paper, in the subsequent simulation using classic MVDR as B_A of Eq. (15), that is the B_{MVDR} of the Eq.(7).

Simulation and analysis

Simulation Model

In May 1993, the Naval Research Laboratory presented several typical shallow sea environment models and the simulation data for the researchers to use during the seminar[11]. Its purpose is in order to be able to compare performance of the different environment matched field inversion and positioning algorithm objectively and fairly. "Genlmis" is used to verify the performance of the algorithm in the presence of colored noise environment and with parameter mismatch; it is a simulation case of severe mismatch. In this paper, the simulation and analysis is based on the data.

A vertical linear array with 20 sensors is used to receive signal in the simulation, the sound source frequency is 250 Hz. The depth of first sensor is 5 m, the depth of last sensor is 100 m, with 5 m equal spacing. The Kraken normal mode model is used to calculate the replica vector. The distance of the observation area from 5 km to 10 km, distance step 20 m; depth from 1m to 100 m, depth step 1m.

The real environment parameter model "genlmis" is shown in Figure 1, that iuses this environment model to construct measured field. There are 3 kinds of sound source under this environment: (1) sound source is located at (6.2 km, 92 m), SNR is 40 dB; (2) sound source is located at (9.0 km, 74 m), SNR is 10 dB; (3) sound source is located at (7.2 km, 16 m), SNR is -5 dB.

Simulation result without environment mismatch

Assume the sound source is located at (9.0 km, 74 m), the SNR is 10 dB, the accurate environment parameter model is shown in Figure 1. The Bartlett, MVDR and MFP-CPC is used to do match field processing respectively, the slices of the source is show in Figure 2.These 3 kinds of MFP can pinpoint

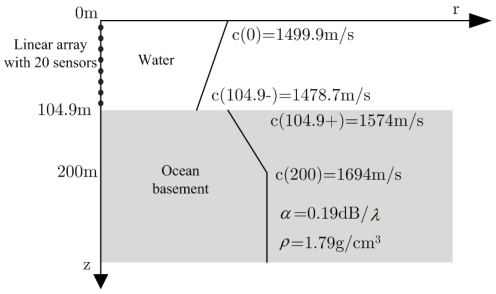

Fig. 1 — GENLMIS real environment model

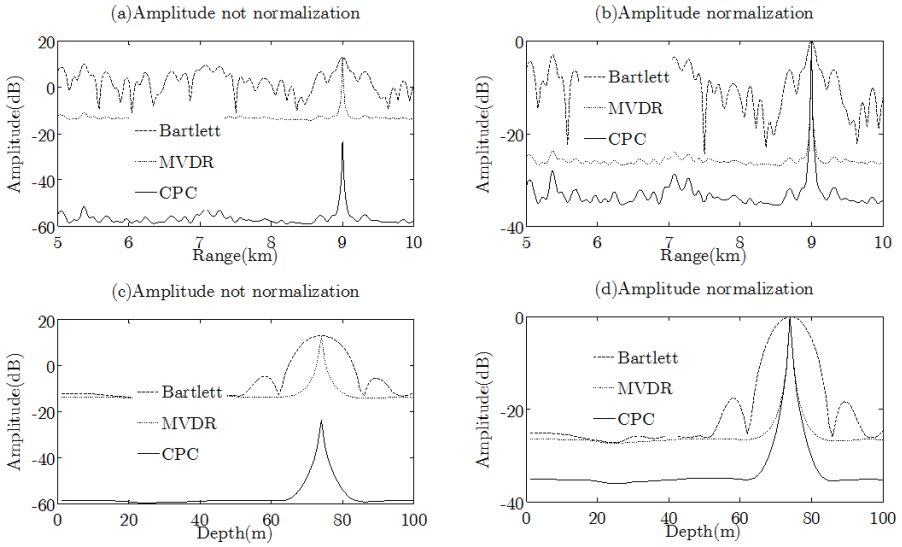

Fig. 2 — Slices of localization results for the 3 MFP methods

the target successful according to the results in Figure 2, the MVDR and MFP-CPC has the more narrow mainlobe and lower sidelobe. When the number of sensors N is 20 and exactly match the theory output power of the MFP is $10\lg(N)=13\text{dB}$, in figure 2(a) and 2(c), the output power of Bartlett and MVDR at (9.0 km,74 m) are approximate 13 dB, agree with the theoretical value. But the output power of MFP-CPC is far less than the two before, the main reason is that the posteriori probability has an influence on the output of MFP.

The comparison for the results after amplitude normalization of the three kinds of processor is shown in Figure 2 b and d. The mainlobe of MFP-CPC and MVDR coincide, the -3d B mainlobe width for the distance is all 20 m, the -3d B mainlobe width for the depth are all 1.5 m, but the Bartlett's mainlobe width for the distance and depth is 100 m and 7 m respectively. In Figure 2(b), for the distance, the highest sidelobe of MVDR is about 35dB less than the Bartlett and the highest sidelobe of MFP-CPC is about 6 dB less than MVDR; In Figure 2(d), for the depth, the sidelobe of MVDR and MFP-CPC are not able to be distinguished, they are lost in the background. The background of MVDR is about 24 dB less than the highest sidelobe of Bartlett and the background of MFP-CPC is about 8 dB less than the background of MVDR.

From the simulation result without environment mismatch，it is clear that the localization performance of MFP-CPC is much better than the Bartlett, the mainlobe of MFP-CPC is same as MVDR, and the sidelobe of MFP-CPC is about 6 dB less than MVDR, the background of MFP-CPC is about 8 dB less than MVDR.

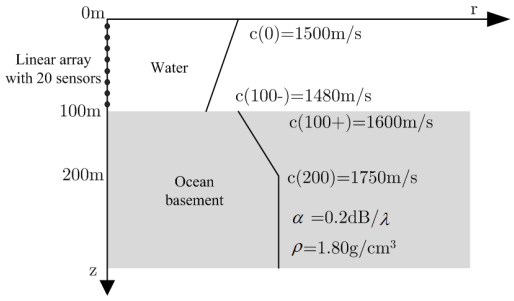

Fig. 3 — GENLMIS environment model with mismatch

Simulation result with environment mismatch

The measured field is still calculated by the environment parameter model as shown in Figure 1. We assume the geoacoustic parameters are unknown and only the prior knowledge about the environment parameters are empirically estimated, as shown in Figure 3. Compared with the real environment model shown in Figure 1, the sound velocity of the surface of ocean mismatch is -0.1 m/s, the sound velocity of the bottom of ocean mismatch is -1.3 m/s, the sound velocity of the upper surface of ocean basement mismatch is -26 m/s, the sound velocity of the middle of ocean basement mismatch is -56 m/s, the sound velocity of the bottom of ocean basement mismatch is -56 m/s, the attenuation coefficient of the ocean basement mismatch is -0.01d B/λ, the density of the ocean basement mismatch is -0.01 g/cm^3, depth of the sea mismatch is 4.9 m, and there is colored noise in the measured field data of "genlmis" model.

Under the “genlmis” model with environment parameters mismatch, the ambiguity surface of the location result by the 3 kinds of MFP for the 3 sound sources as introduced in simulation model section and is shown in Figure 4. Classified according to the type of MFP: Figure 4 (a,b,c) are the location results of Bartlett; Figure 4 (d,e,f) are the location results of MVDR; Figure 4 (g,h,i) are the location results of MFP-CPC. Classified according to the sound source: Figure 4 (a,d,g) are the location results of first sound source with 40 dB SNR; Figure 4 (b,e,h) are the location results of second sound source with 10 dB SNR; Figure 4 (c,f,i) are the location results of third sound source with -5 dB SNR. The mainlobe value in the small rectangular box in each sub image is the estimation of sound source location by the 3 kinds of MFP in Figure 4.

When the SNR is 40 dB and 10 dB, the Bartlett and MFP-CPC give the correct location results, but in the ambiguity surface of Bartlett, there is many sidelobe’s amplitude close to the mainlobe’s. In Figure 4(a) the mainlobe at (6.2 km, 92 m) is bigger than the maximum sidelobe at (8.2 km, 92 m) less than 2 dB; and in Figure 4(b) the mainlobe at (9.1 km, 72 m) is bigger than the maximum sidelobe at (7.2 km, 70 m) less than 1dB, and thus it is very hard to distinguish. But in Figure 4(g), the mainlobe of MFP-CPC is about 6dB bigger than the maximum sidelobe. In Figure 4(h), the maximum sidelobe is located at (7.7 km, 16 m), and is not same as the position of the maximum sidelobe in Figure 4(b), as it can be seen because of the infulence of MVDR from Figure 4(e); and in Figure 4(h), the mainlobe at (9.1 km, 71 m) is still about 3 dB bigger than the maximum sidelobe indicating obviously that the MFP-CPC’s sidelobe compression performance is better. MVDR has severe "suppression" phenomenon under the condition of the 2 kinds of SNR, there are many peaks that appear at the surface of the sea suggecting that the MVDR is most sensitive to environmental mismatch, but the good thing is that the peak still can be seen at the real sound source location. When the SNR is -5 dB, and all the 3 kinds of MFP failure occur at this time, the influence of colored noise and environmental mismatch is most obvious, and the positioning of the false target is blurred by MVDR. Although the Bartlett and MFP-CPC only have false targets at (6.5 km, 16 m), but the false targets are clear. In contrast the location results of Bartlett and MFP-CPC can be seen such that even in serious mismatch cases, their ambiguity of the location results near the real target also have a certain similarity, that is they have similar robustness.

Verification by ocean experimental data

Experiment parameter

The ocean near the north island of Elba of the west coast of Italy is a typical shallow water environment,

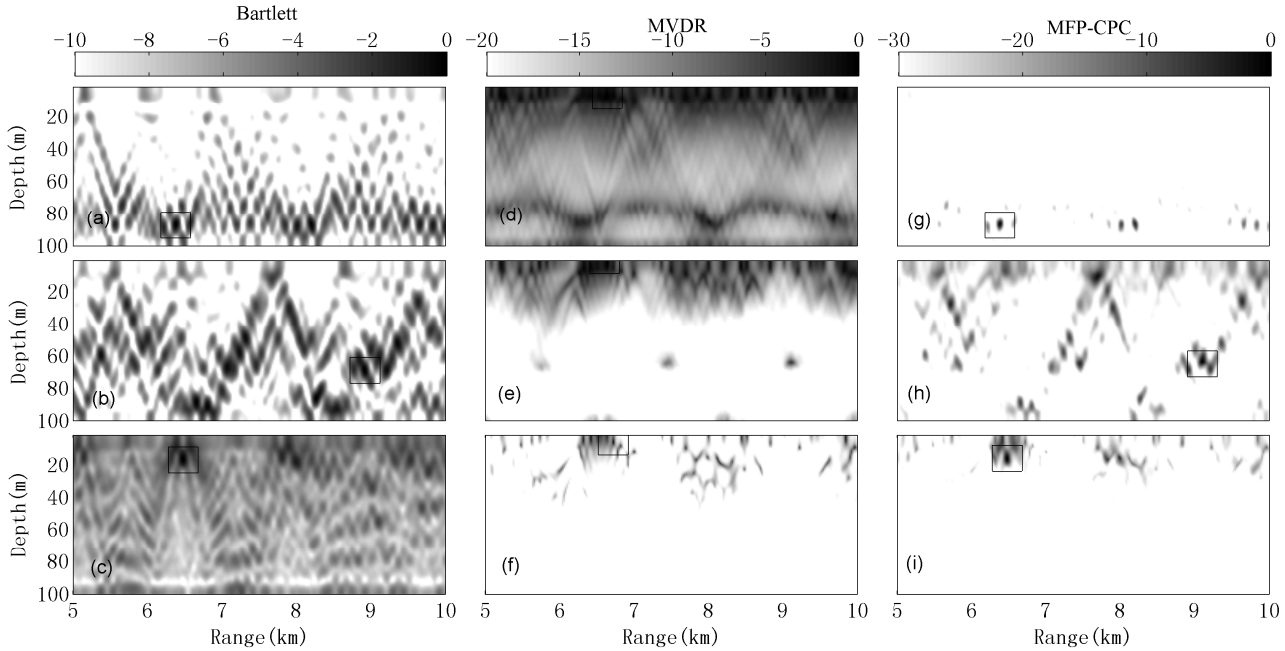

Fig. 4 — Localization results for the 3 MFP methods under GENLMIS environment model

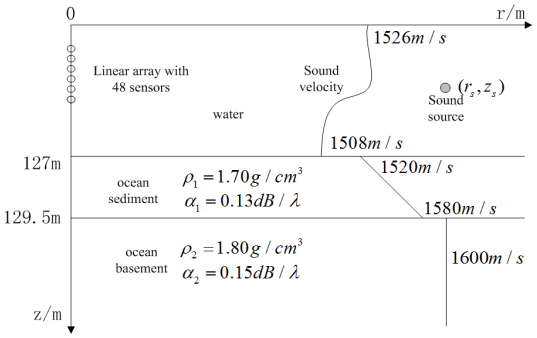

Fig. 5 — Environmental model in shallow water

On October 26 and 27, 1993, the SACLANT Research Center did ocean experiment for two days at the ocean[17]. In this paper, we use the experimental data to do processing and analysis. The array and environment parameters for the experiment are described in Figure 5. The bathymetry (125.5-128.5 m); upper sediment sound-speed (1450-1550 m/s); lower sediment sound-speed (1500-1600 m/s); sediment density (1.2-2.2 g/cm3); sediment attenuation (0.0-0.4 dB/λ); sediment thickness (0.0-0.6 m); sub-bottom sound-speed (1550-1650 m/s); sub-bottom density (1.2-2.2 g/cm3); sub-bottom attenuation (0.0-0.4 dB/λ).

During the experiment on October 26, sound source moored in 5500 ± 200 m distance from the receiving array, the depth is about 79 m. On October 27, sound source was towed by a tugboat with 3 km speed, navigation in a straight line. The depth is about 65 m, the initial distance from the receiving array is about 5.9 km. The experiment collected the signals received from the linear array for 10 minutes. During the two days experiment, the acoustic signal models were slightly different. On October 26, the signal was continuous, and on October 27, the signals were not continuous. They were on for 30 out of every 60 sec. We used the experimental data to verify the performance of the MFP-CPC.

According the Eq. (4), we used the data of first 25 seconds to make 25 snapshots, the average of these snapshots is the maximum likelihood estimation of sampling covariance matrix. The length of the snapshot is 2 seconds, the overlap between the two snapshots is 50 %, for 1 kHz sampling rate, each snapshot contains 2000 sampling points.

Results of experimental data

The location result of the moored source at the first minute is shown in Figure 6. The rectangle area is the position of the peak amplitude on the ambiguity

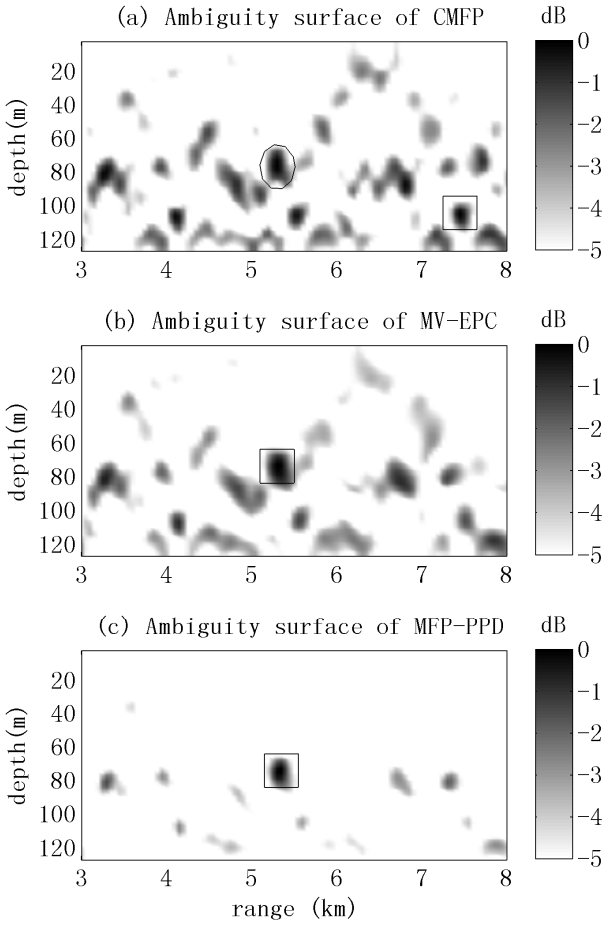

Fig. 6 — Ambiguity surfaces of moored source at the first minute

surface, it is also the location result of the MFP, the ellipse area is the position of real target, and we only draw a rectangle when the ellipse and rectangle overlapped. If the peak amplitude position of the ambiguity surface is near the real target (depth around ± 10 m, distance around ± 500 m), that suggests the localization success.

It is clear that the location result of Bartlett is wrong in Figure 6(a), the error result is (104.7 m, 7450 m), and there is also a peak at the real position. The location result (73.5 m, 5300 m) of MVDR is shown in Figure 6(b), it is correct, but the amplitude of the sidelobe is a little bit higher, only around 1 dB lower than the mainlobe. Figure 6(c) is the ambiguity surface of MFP-CPC, where we can clearly find the target and there is no confusion between the target and sidelobe.

The slices of the moored sources at the first minute are shown in Figure 7, under the real uncertain environment, the Bartlett is failed to localize, thus we only compare the results of MVDR and MFP-CPC.

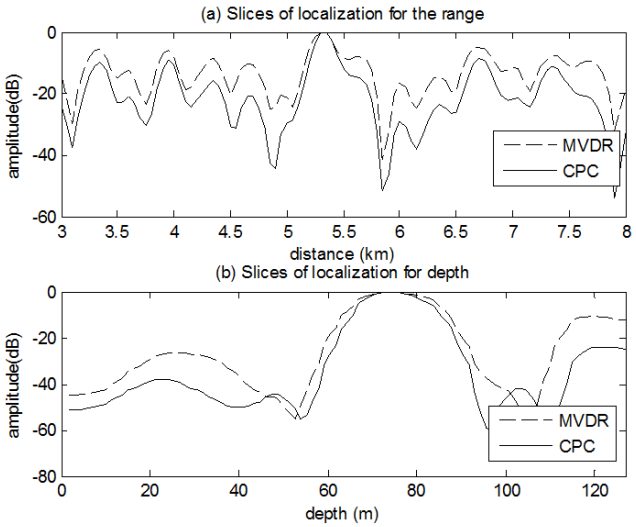

Fig. 7 — Slices of the moored source at the first minute

Table 1 — Results of the moored source at the second minute

Processor	Location results			
	z(m)	r(m)	SINR(dB)	PBR(dB)
CMFP	76.1	5300	10.70	5.41
MV-EPC	74.8	5300	11.57	6.49
MFP-PPC	74.8	5350	14.32	9.16

From the Figure 7 (a,b), it is clear that the MFP-CPC has more narrow mainlobe and lower sidelobe. The location results of 2 to 10 minutes are similar to the result of first minute, the main difference is that the Bartlett give the correct results at 2, 5, 7, 8 minutes, the location results are all around (76.1 m,5300 m). Both MVDR and MFP-CPC give the correct results during the 10 minutes, the results are same as in first minute.

In order to make quantitative evaluation for the three kinds of MFP, we introduce two parameters for performance evaluation, one is signal to interference noise ratio (SINR), the other is peak to background ratio (PBR). The SINR quantize the differentiation between the mainlobe and sidelobe, it will be easier to distinguish mainlobe from sidelobe when the SINR is bigger; the PBR quantize the differentiation between the mainlobe and background, it will be easier to find out the mainlobe when the PBR is bigger.

We make quantitive comparison for the location results of the three kinds of MFP at the second minute in Table 1. For the depth localization, the result of Bartlett is more close to the target depth, but the result difference to the other two processors is only a depth of a grid. For the distance localization, the results are same for the three processors, but the SINR and PBR

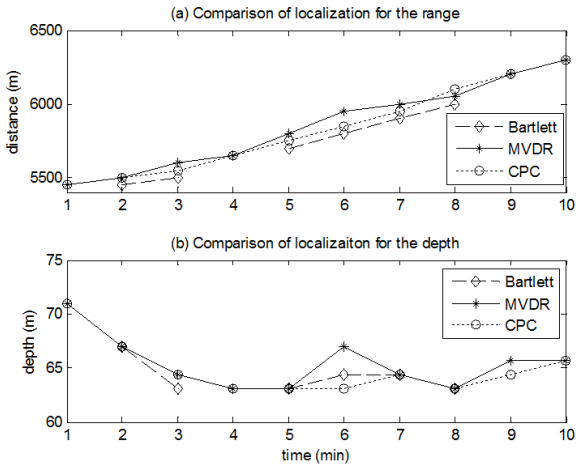

Fig. 8 — Tracking of the moving source in the whole ten minutes

of the MVDR are about 1 dB higher than the Bartlett, and the SINR and PBR of the MFP-CPC are about 2.5 dB higher than the MVDR. From the numerical results of the moored source at the second minute, we can see that MFP-CPC has optimal localization performance, followed by the MVDR, and the Bartlett is the worst.

The curve of localization results of the moving source in 10 minutes on October 27 is shown in Figure 8. During the 10 minutes, the Bartlett give the correct results at 2, 3, 5, 6, 7, 8 minutes, other time failed, the error localization results are not shown in Figure 8. The MVDR and MFP-CPC give the correct results in the whole 10 minutes, and we can see that the motion curve of MFP-CPC is more like a uniform linear motion as shown in Figure 8.The slope of the curve of MFP-CPC is about 1.6 m/s, and the MFP-CPC is best consistent with the speed and trajectory of the moving source.

The distance localization result is around 500 m closer than the real target as shown in Figure 8(a), perhaps due to the reason that the water depth around source is 13 m deep than 127 m as discussed in details in the article[17]. The distance localization result of this article is equal to the article[17]. In Figure 8(b), the depth localization results of the three processors at first minute are around 71 m, 6 m error, at 6th minute, the error of MVDR is about 3 m, the error of the other two processor is 1m, at the other time, the depth localization error of the three processors are all within 2 m. Because the moving source is towed behind the ship, for the first and second minutes, at the beginning of the movement, the tension of the cable which connect the source is too small and unstable, thus causes the deep source. During this period, the depth

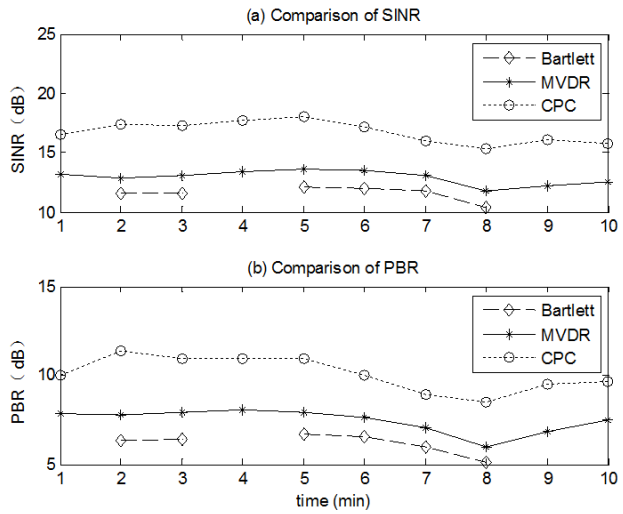

Fig. 9 — Localization performance for the moving source

localizaiton results of the three processors are same, so we can consider that the depth of source is about 71m. For the 6th and 9th minute, since the tugboat was moving smoothly, the depth localization difference of the three processors is mainly due to the ups and downs of sea waves; the uncertainty of the environment and array element position error. Under this condition, the localization performance is heavily dependent on the robustness of the algorithm. It is clear that the localization result of MFP-CPC is more accurate than MVDR, and the Bartlett is failed at 9th minute.

The SINR curve for the moving source in the 10 minutes is shown in Figure 9(a), when given the correct localization results, the SINR of MVDR is about 1.5 dB higher than Bartlett, and the SINR of MFP-CPC is about 3 dB higher than MVDR. The PBR curve for the moving source in the 10 minutes is shown in Figure 9(b), the PBR of MVDR is about 1.7 dB higher than Bartlett, the PBR of MFP-CPC is about 3 dB higher than MVDR. So not only it is easiest to distinguish mainlobe from sidelobe by the MFP-CPC, but also the mainlobe and background difference is largest in MFP-CPC. It is clear that the MFP-PCPC has the best localization performance as shown in Figure 9.

Conclusion

It is easy to appear mismatch between the building environment model and the real environment when doing MFP because of the uncertainty of prior environment information, that eventually lead to serious performance loss of MFP, especially when doing AMFP. In order to solve this problem, a Conditional Probability Constraint Matched Field Processing (MFP-CPC) is proposed. The MFP-CPC algorithm derives the posterior probability density of the source locations by the field measurement data received by the vertical array, and then use the posterior probability density to protect the mainlobe of AMFP and restrict the sidelobe. From the simulation results without environment mismatch，it is clear that the mainlobe width of MFP-CPC is same as MVDR, and the sidelobe of MFP-CPC is about 6-8 dB less than MVDR. From the simulation results with environment mismatch，it is clear that the MFP-CPC and Bartlett have similar robustness.

For typical uncertain shallow environment, the analysis result of ocean experimental data of the moving sound source showed that: MFP-CPC can restrain location errors which are caused by physical factors like the wind and waves, the array element position, and movement of the source, especially in the process of tracking for 10 minutes, the range and position curve accord well with the moving trail of the sound source.

In addition, the conditional probability constraints algorithm is relatively simple, and the expression is versatile and general, the adaptive unit of the algorithm can be replaced by the other adaptive algorithm, so as to further improve the robustness of the algorithm. But when calculating the posterior probability estimates that still needed to use a priori environmental information, so the mismatch problems also exist, and as compared to the AMFP used in the algorithm, the robustness is improved.

Competing Interests

The authors declare that they have no competing interests.

Acknowledgment

Supported by “the Fundamental Research Funds for the Central Universities”（3102017zy010）

References

1 Porter, M. B. The Kraken normal mode program [R]. La Spezia Italy, 1992.

2 Baggeroer, A.B., Kuperman, W.A. & Mikhalevsky, P.N. An overview of matched field methods in ocean acoustics. *IEEE J. Oceanic Engg.*, 18(4) (1993) 401-424.

3 You, Wei, He Zi-shu, & Hu Jin-feng,. Skywave radar altitude estimation algorithm based on matched-field processing. *J. Electron. Inform. Technol.*, 35(2) (2013) 401-405.

4 Mantzel, W., Romberg, J. & Sabra, K. Compressive matched-field processing. *J. Acoust. Soc. America*, 132(1) (2012) 90-102.

5 Shorey, J.A., Nolte, L.W. & Krolik, J.L. Computationally efficient Monte Carlo estimation algorithms for matched field processing in uncertain ocean environments. *J. Comput. Acoust.*, 2(3) (1994) 285-314.

6 Singh, V., Knisely, K.E. & Yönak, S.H., *et al.* Non-line-of-sight sound source localization using matched-field processinga. *J. Acoust. Soc. America*, 131(1) (2012) 292-302.

7 Teyan, C., Chunshan, L. & Zakharov, Y.V. Source localization using matched-phase matched-field processing with phase descent search. *IEEE J. Ocean. Engg.*, 37(2) (2012) 261-270.

8 Zhuan, X., Wen, X. & Xianyi, G. Robust matched field processing for source localization using convex optimization. *OCEANS '09 IEEE Bremen: Balancing Technology with Future Needs, Bremen Germany*, 2009: 1-5.

9 Schmidt, H., Baggeroer, A.B. & Kuperman, W.A., *et al*. Environmentally tolerant beamforming for high-resolution matched field processing: deterministic mismatch. *J. Acoust. Soc. America*, 88(4) (1990) 1851-1862.

10 Chandler, H.A., Feuillade, C. & Smith, G.B. Sector-focused processing for stabilized resolution of multiple acoustic sources. *J. Acoust. Soc. America*, 97(4) (1995) 2159-2172.

11 Porter, M.B. & Tolstoy, A. The matched field processing benchmark problems. *J. Comput. Acoustics*, 2(3) (1994) 161-185.

12 Liu Feng-xia, Pan Xiang, & Gong Xian-yi. Matched-field three-dimensional source localization using spiral line array. *J. Zhejiang Univ. (Engg. Sci.)*, 47(1) (2013) 62-69+76.

13 Yang, K., Zhang, T. & Ma, Y. Matched-field processing using time-reversal concept in a range-dependent environment. *J. Acoust. Soc. America*, 131(4) (2012) 3239-3239.

14 Krolik, J.L. Matched-field minimum variance beamforming in a random ocean channel. *J. Acoust. Soc. America*, 92(3) (1992) 1408-1419.

15 Lee, N., Zurk, L.M. & Ward, J. Evaluation of reduced-rank, adaptive matched field processing algorithms for passive sonar detection in a shallow-water environment. *Conference Record of the Asilomar Conference on Signals, Systems and Computers. United States*, 2(1999) 876-880.

16 Bretthorst, G.L. The maximum entropy method of moments and Bayesian probability theory. *32nd International Workshop on Bayesian Inference and Maximum Entropy Methods in Science and Engineering, Garching, Germany*, 2012: 3-15.

17 Krolik, J.L. Robust matched-field beamforming with benchmark shallow-water acoustic array data. *IEEE International Conference on Acoustics, Speech, and Signal Processing, 1996. ICASSP-96*. 1996, 1185-1188 vol. 2.